ELSEVIER

Deep-Sea Research II 52 (2005) 1270–1286

DEEP-SEA RESEARCH
PART II

www.elsevier.com/locate/dsr2

Momentum and energy exchange across an air–water interface. Partitioning (into waves and currents) and parameterization

Y.A. Papadimitrakis

Water Resources, Hydraulics & Maritime Engineering Division, National Technical University of Athens (NTUA), School of Civil Engineering, 5 Heroon Polytechniou St., Zografos Campus, Zografos, 15780 Athens, Greece

Accepted 17 January 2005

Abstract

Expressions have been derived to parameterize: (a) the total (time) mean wind momentum and energy fluxes across the air–sea interface, and (b) their partition into waves and a mean surface drift current, as expressed by the fractions γ_M and γ_E, in terms of the wave age, c_p/u_*, and the significant slope, §, of the wave field. Available laboratory and field observations support the parameterization predictions. The fraction of the wave-supported momentum,γ_M, increases initially with the wave age (and/or the non-dimensional fetch, $\tilde{x}$) but, as the wave field matures, it diminishes and attains rather constant small values (of about 0.05) at large wave ages (and/or $\tilde{x}$). For a fixed wave-age (and/or $\tilde{x}$), γ_M, increases with §. The corresponding wave-supported energy fraction, γ_E, shows a similar behavior for small and moderate wave ages (and/or $\tilde{x}$), although γ_E values remain greater than about 0.5 in the range $5 \leqslant c_p/u_* \leqslant 10$; yet, at larger wave ages (and/or $\tilde{x}$), although γ_E values remain greater than about 0.5 in the range $5 \leqslant c_p/u_* \leqslant 10$; yet, at larger wave ages (and/or $\tilde{x}$) γ_E appears to increase again, reaching values of about 0.8 when $c_p/u_* \approx 30$, features, all in accord with experimental observations. For waves generated locally by wind, where c_p/u_* is of O(1), a significant portion of the normalized total (time) mean wind-energy flux across the interface goes directly to the surface drift current, the remaining being transferred to the waves. For mature waves or waves generated in the presence of swell, where c_p/u_* is of O(10), this energy partition changes, the waves now supporting more energy than the surface drift current. The relative importance of the normalized wave-energy dissipation fraction, compared with the corresponding wave-energy fraction advected by the wave field and the energy fraction supported by the drift current, is also examined as the wave field develops.

1. Introduction

Parameterizing the total (time) mean wind momentum and energy fluxes across the atmosphere–ocean interface has received little attention thus far, although understanding of many physical processes resulting from air–sea interactions requires quantitative knowledge of the partition of these fluxes into waves and a mean surface drift current.

E-mail address: ypapadim@central.ntua.gr.

0967-0645/$ - see front matter © 2005 Elsevier Ltd. All rights reserved.
doi:10.1016/j.dsr2.2005.03.006

Most often in studies of the dynamics of the upper ocean (Phillips, 1977), the total wind momentum and energy fluxes from the atmosphere to the ocean are taken as $\rho_a u_*^2$ and $\rho_a u_*^3$, respectively, where u_* is the wind friction velocity and ρ_a is the air density; now we learn differently, however (cf. Section 4). It also has been assumed that some fraction of these quantities goes into the surface waves, the remaining being transferred to the surface drift current. For estimating the wave-supported momentum and, in fewer cases, the wave-supported energy as a fraction of either $\rho_a u_*^2$ or $\rho_a u_*^3$ some investigators have used simplified transport mechanisms (e.g., Donelan, 1979; Mitsuyasu, 1985; Eiffler, 1993; Bye and Wolff, 2001). Others have calculated the wave-supported fluxes, along with other important air–sea interaction parameters, either simulating numerically the behavior of the atmospheric boundary layer under neutral and/or thermally stratified conditions (e.g., Chalikov and Makin, 1991; Jenkins, 1992; Makin and Kudryavtsev, 1999; Bye and Wolff, 1999), or with the aid of integral theories of the interaction of waves with the wind (Hsu et al., 1982; Papadimitrakis et al., 1986a).

Laboratory and field work, in this area, has been conducted by various investigators during several decades, and more specifically by Donelan (1979), Snyder et al. (1981), Hsu et al. (1982), Hsiao and Shemdin (1983), Papadimitrakis et al. (1986a), Katsaros et al. (1993), Donelan et al. (1997), Banner and Peirson (1998), Atakturk and Katsaros (1999) and Grachev and Fairall (2001). Among these observations only a few correspond to the water proximity, a region that certainly controls all of the transport processes. Such data have been collected either in an Eulerian, wave-following, frame of reference—although they do not belong to the viscous sublayer region (e.g., Snyder et al., 1981; Hsiao and Shemdin, 1983; Papadimitrakis et al., 1986a), or by means of other sophisticated techniques. Banner and Peirson (1998), for example, using VIP techniques for investigating, in a laboratory flume, the structure of the thin shear layer just beneath a wind-driven air–water interface, presented results on the contribution of surface shear stresses (tangential and normal to the surface wave form, in their terminology) in transmitting the atmospheric wind-stress into the water motion. They further studied the behavior of the wave-modulated part of the tangential component of the surface shear stress as the wave field progressively matured.

Examination of the available laboratory and field observations on the *conventionally defined fraction of momentum flux* to the waves (or the wave-supported momentum flux as a fraction of the surface stress), $r_M = \tau_w/\tau_0$, where τ_w represents the wave-supported part of the wind-stress $\tau_0 (= \rho_a u_*^2)$, indicates that wide discrepancies exist among the corresponding results of these investigations. The literature data indicate that the fraction r_M varies from a few percent to almost 100%. For large fetches r_M appears to be small ($\leqslant 10\%$), whereas for small fetches r_M appears to be large (60–100%).

Regardless of the apparent and real differences among the available observations on the wave-supported wind momentum (and energy fluxes), there has not been (at least, to our knowledge) any systematic effort to parameterize these fluxes (however they are defined) and their partition into waves and a mean drift current in terms of widely accepted and readily determined parameters. This is the subject of the present paper.

2. Momentum and energy exchange mechanisms

A detailed description of the mechanisms involved in the process of exchanging wind momentum and energy across the air–sea interface (under thermally neutral conditions), and their relative importance, can be found in Papadimitrakis et al. (1986a), although other investigators (e.g., Hsu et al., 1982; Chalikov, 1985) provide similar descriptions. Briefly, the horizontal (time) mean shear stress acting against the (time) mean wind-velocity gradient (in the vertical direction) draws energy from the (time) mean wind field and transfers it to both the wave-perturbed and turbulent (wind) fields. This energy, in turn, is transmitted through the action of wave-induced pressure and wave-induced Reynolds stresses, in the air, to the surface waves and, via the action of (time) mean static pressure and turbulent normal

and shear stresses (again in the air), to the surface drift current. For definitions of the respective quantities and a detailed description of the contribution of the above agents to the momentum and energy transfer processes across an air–sea interface (under various sea state but thermally neutral atmospheric conditions), the interested reader should peruse Hsu et al. (1982) and Papadimitrakis et al. (1986a).

Briefly, neglecting the transport by viscous stresses, the total (time) mean wind momentum and energy fluxes, $\bar{M}_{\mathrm{T}}$ and $\bar{E}_{\mathrm{T}}$, transferred across the interface are given by Eqs. (2.5–2.10) of Papadimitrakis et al. (1986a). These expressions have been derived by integrating vertically the boundary-layer momentum and energy equations in the air, held in an Eulerian wave-following coordinate system that contains only vertical translation, and are exact for two-dimensional flows. However, similar expressions have been given by Hsu et al. (1982) for three-dimensional flows. We therefore, following Hsu et al. (1982) and Papadimitrakis et al. (1986a), characterize the partition of total (time) mean wind-momentum flux into waves and a mean drift current by the ratio $\gamma_{\mathrm{M}}(=\bar{M}_{xw}/\bar{M}_{x})$ of (time) mean wave-supported momentum in the mean wind direction x–x, $\bar{M}_{xw}$, and the total (time) mean momentum, $\bar{M}_{x}$, transferred across the interface in the same direction. Similarly, we characterize the partition of total (time) mean energy flux into waves and a mean drift current by the ratio $\gamma_{\mathrm{E}}(=\bar{E}_{\mathrm{w}}/\bar{E}_{\mathrm{T}})$ of (time) mean energy transfer from the wind to waves, $\bar{E}_{\mathrm{w}}$, and the total (time) mean energy transferred across the interface, $\bar{E}_{\mathrm{T}}$. Again, we understand that the ratio $r_{\mathrm{M}}=\tau_{\mathrm{w}}/\tau_{\mathrm{o}}$ may not be equivalent to γ_{M} (see also Section 4).

With this picture in mind, it will be attempted to parameterize: (i) the total (time) mean wind momentum and energy fluxes transferred to the water side, and (ii) their partition into waves and a mean (drift) current, given by the fractions γ_{M} and γ_{E}, in terms of commonly used parameters that express the wind-field and sea-state conditions and their mutual coupling, under thermally neutral conditions in the absence and/or presence of swell. Such parameters are the significant slope, the wave age and the swell slope. The definitions of various quantities follow in proper sections and in the appendix.

3. A micro-scale model for the momentum and energy fluxes

3.1. The Energy Transfer Equation

For accomplishing the objectives of this study, use has been made of: (a) an integral form of the wave energy balance equation in deep water (known also as radiative-transport equation, cf. Hasselmann et al., 1976), and (b) of various correlations that describe the spatial development of the wave field and the (local) wave energy losses caused by the various dissipative mechanisms.

The generation of waves by the wind includes three distinct stages of development characterized, respectively, by wave growth, equilibrium, and decay. These wind–wave interaction processes[1] can be accurately described by the wave energy balance equation, which for deep water takes on the form:

$$\frac{\partial F(\sigma,\phi)}{\partial t}+\{c_{\mathrm{g}}(\sigma,\phi)+u_{\mathrm{ds}}\}\nabla F(\sigma,\phi) = w(\sigma,\phi)+\ell(\sigma,\phi)+\mathrm{i}(\sigma,\phi). \tag{3.1}$$

Here, $F(\sigma,\phi)$ is the two-dimensional wave energy spectrum and the symbol ∇ represents the horizontal gradient operator; $c_{\mathrm{g}}(\sigma,\phi)$ is the group velocity of the wave component with frequency σ propagating at an angle ϕ with respect to the streamwise mean wind, x–x, direction, and the angle φ is measured clockwise from the $(-x)$ direction; u_{ds} is a Eulerian mean velocity representative of the surface drift current. A procedure to determine u_{ds} is described, in detail, in the appendix. $w(\sigma,\phi)$, $\ell(\sigma,\phi)$ and $i(\sigma,\phi)$ are, respectively, the source functions of wind-energy input to the waves, wave-energy dissipation, and energy transfer among the wave components of the spectrum via the nonlinear wave–wave interaction mechanism. In general, $F(\sigma,\varphi)$ is a function of the

[1]In this work, we consider only dispersive wave trains, since the description of non-dispersive bound wave trains requires a different approach.

position vector and time, t; it can be approximated by the product of the one-dimensional spectrum, $\Phi(\sigma)$, and the normalized directional spreading factor $D(\phi)$ or $D(\sigma,\phi)$. The directional wave spectrum, $F(\sigma,\varphi)$, proposed by Donelan et al. (1985), and modified slightly by Banner (1990), has been used in the subsequent calculations.

Now integrating Eq. (3.1) with respect to φ, from $-\pi$ to π (neglecting back scattering effects, at least for laboratory waves), we obtain:

$$\frac{\partial\Phi(\sigma)}{\partial t}+\{\bar{c}_{\mathrm{g}}(\sigma)+u_{\mathrm{ds}}\}\frac{\partial\Phi(\sigma)}{\partial x} = W'(\sigma)+L'(\sigma)+I'(\sigma), \tag{3.2}$$

$$\bar{c}_{\mathrm{g}}(\sigma)=\left[\int_{-\pi}^{\pi}c_{\mathrm{g}}(\sigma,\phi)\cos\,\varphi F(\sigma,\phi)\,\mathrm{d}\varphi\right]\times\left[\int_{-\pi}^{\pi}\int_{0}^{\infty}F(\sigma,\varphi)\,\mathrm{d}\sigma\,\mathrm{d}\phi\right]^{-1}, \tag{3.3}$$

where $\bar{c}_{\mathrm{g}}(\sigma)$ is the directionally averaged group velocity in the mean wind ($+x$) direction. An expression for $c_{\mathrm{g}}(\sigma,\varphi)$ ($=\partial\sigma/\partial k$, where k denotes wave number), including drift current and swell effects, can be obtained from the kinematical conservation equation and other dynamic considerations (Papadimitrakis, 1986). $W'(\sigma)$, $L'(\sigma)$ and $I'(\sigma)$ are integrals of $w(\sigma,\phi)$, $\ell(\sigma,\phi)$ and $i(\sigma,\phi)$ with respect to φ, from $-\pi$ to π.

Integrating (3.2) over all frequency components, we obtain:

$$\frac{\partial E_{\mathrm{w}}}{\partial t}+\{\bar{C}_{\mathrm{g}}+u_{\mathrm{ds}}\}\frac{\partial E_{\mathrm{w}}}{\partial x}=W-L, \tag{3.4}$$

$$E_{\mathrm{w}}=\rho g\int_{0}^{\infty}\Phi(\sigma)\,\mathrm{d}\sigma=\rho g\overline{\eta^2},$$
$$W=\rho g\int_{0}^{\infty}W'(\sigma)\,\mathrm{d}\sigma,$$
$$L=-\rho g\int_{0}^{\infty}L'(\sigma)\,\mathrm{d}\sigma, \tag{3.5a, b, c}$$

where E_{w} is the total wave energy, ρ is water density, g is gravitational acceleration, η is the sea surface displacement from the mean water level (MWL), and $\bar{C}_{\mathrm{g}}$ is an overall mean (wave) group velocity defined as:

$$\bar{C}_{\mathrm{g}}=\left[\int_{0}^{\infty}\bar{c}_{\mathrm{g}}(\sigma)\Phi(\sigma)\,\mathrm{d}\sigma\right]\left[\int_{0}^{\infty}\Phi(\sigma)\,\mathrm{d}\sigma\right]^{-1} \tag{3.6}$$

The second term on the LHS of (3.4), denoted as R, represents the rate of transport of energy by the waves and is associated with the spatial and/or temporal wave growth. W is the total energy input to the waves (from the wind), and L is the total wave-energy dissipation rate. The nonlinear wave–wave interactions conserve energy and, therefore, have a zero net effect on the total wave-energy balance. Consequently, from the latter point of view, only the wind-energy input, W, the wave growth (or decay), R, and the wave-dissipation losses, L, are relevant mechanisms in the evolution of a wave field.

Next, we determine the rates of wind-energy input to the waves and to the mean drift current, as well as the rate of energy dissipation from the waves (mainly to turbulence) during the developing stage. The decaying stage is not considered in this work, for both the spatial rate of wave decay, and the rate of wave-energy dissipation require special treatment.

3.2. Energy flux into the wave field

When $W>L$ the waves will grow. Since we are interested in determining the total wave-energy balance, (3.4) may be rewritten as:

$$W=\frac{\partial E_{\mathrm{w}}}{\partial t}+\{\bar{C}_{\mathrm{g}}+u_{\mathrm{ds}}\}\frac{\partial E_{\mathrm{w}}}{\partial x}+L. \tag{3.7}$$

Under steady-state conditions, the first term on the RHS is zero. The second term can be determined from knowledge of the wave growth with fetch. Experimental observations, under field (e.g., Kahma and Calcoen, 1992; Babanin and Soloviev, 1998; Young, 1997) and laboratory conditions (e.g., Huang et al., 1981; Hsu et al., 1982), indicate that a relation between the non-dimensional wave energy, $\tilde{E}_{\mathrm{w}}\{=E_{\mathrm{w}}/(\rho u_*^4/g)\}$, and the non-dimensional fetch, $\tilde{x}(=gx/u_*^2)$, exists; x here denotes fetch. This relationship, however, may be different for waves generated in the presence or absence of a swell, provided that the corresponding growth rates are different.

In the absence of swell we have:

$$\tilde{E}_w = \kappa\tilde{x}, \quad \tilde{E}_w = \frac{g^2\overline{\eta^2}}{u_*^4}, \tag{3.8a, b}$$

where κ is a coefficient that can be determined from laboratory and/or field observations. Although Hsu et al. (1982) have reported that κ is approximately constant with a value of about 1.6×10^{-4}, Huang et al. (1981), analyzing (fetch-limited) laboratory data taken under various wind conditions (but thermally neutral conditions), concluded that κ is a function of the wave age (c_p/u_*) and the significant slope (§ whose definition is given in the appendix); c_p represents the phase speed of the dominant wave at the spectral peak frequency; the subscript p refers (in general) to the spectral peak. Kahma and Calcoen (1992), reanalyzing field observations collected at three distinct locations (North Sea, Bothnian Sea and Lake Ontario), concluded that under both stable and unstable stratification conditions the dimensionless energy $\tilde{E}_w$ varies almost linearly with the non-dimensional fetch $\tilde{x}$. Under neutral stability conditions, elimination of $\tilde{x}$ in their Eqs. (16–17, letting at the same time the stability parameter to equal zero) produces: $\kappa = 6.485\times10^{-4}(c_p/u_*)^{-0.538}$. Thus, we can derive expressions for R which correspond to both a constant and a variable κ.

Since combining (3.8a, b) yields $E_w = \kappa x(\rho u_*^2)$ and, therefore

$$\partial E_w/\partial x = \kappa\left[1 + 2\,\frac{x}{u_*}\frac{\partial u_*}{\partial x} + \frac{x}{\kappa}\frac{\partial\kappa}{\partial x}\right]\rho u_*^2 = \bar{\kappa}\rho u_*^2 \tag{3.9a, b}$$

it becomes apparent that evaluation of the radiative-transport term, R, requires knowledge of the variation of u_* with fetch. Such information may be obtained from the variation of the wind-stress coefficient, $C_d(=u_*^2/U_\infty^2)$, with fetch; U_∞ is a streamwise (time) mean free-stream wind velocity (a quantity used for laboratory waves, similar to the (time) mean wind velocity, U_{10}, measured at the height of 10 m above MWL in the field). Sinai (1987), among other investigators, using the momentum integral theory in flows above water waves, derived an expression for C_d in terms of $\tilde{x}$, namely:

$$C_d^{-1/2} = \frac{1}{\kappa_0}\ln\{C_0\tilde{x}/C_d^{-1/2}\}, \tag{3.10}$$

where $\kappa_o(\approx 0.4)$ is the Von Karman constant and C_o is a function of several parameters that depend on the structure of the boundary layer developed above the waves. Since for wind-generated waves, both c_p/u_* and § are simple functions of $\tilde{x}$ it is possible to eliminate $\tilde{x}$ from (3.10) and express C_d in terms of either of the latter parameters. Explicit expressions of C_d in terms of the same parameters are also available in the literature, most notably that proposed by Geernaert et al. (1987), viz., $C_{10} = 14.8\times10^{-3}(c_p/u_*)^{-0.738}$, where $C_{10}(=u_*^2/U_{10}^2)$. Such expressions have been derived form field observations and appear to be valid for wave ages greater than 10.

Now in terms of u_* and x, (3.10) yields:

$$\frac{\partial u_*}{\partial x} = -\left\{\frac{u_*}{x}\right\}\left\{\frac{1}{\kappa_0 C_d^{-1/2} - 1}\right\}, \tag{3.11}$$

where C_d maybe evaluated from Sinai's (1987) expression in terms of the wave age. Taking κ to be constant we obtain

$$\frac{\partial E_w}{\partial x} = \bar{\kappa}\rho u_*^2, \quad \bar{\kappa} = \kappa\left\{1 - \frac{2}{\kappa_0 C_d^{-1/2} - 1}\right\}, \quad \kappa = 1.6\times10^{-4}. \tag{3.12a, b, c}$$

Thus, the rate of radiative-transport of the wave energy can be expressed as:

$$R = \{\bar{C}_g + u_{ds}\}\frac{\partial E_w}{\partial x} = \bar{\kappa}(\rho/\rho_a)\{\alpha_1(c_p/u_*) + \alpha_0\}\rho_a u_*^3 = A_1\rho_a u_*^3. \tag{3.13a, b, c}$$

Here we have replaced u_{ds} by $\alpha_0 u_*$ and $\bar{C}_g$ by $\alpha_1 c_p$, where the coefficients α_0 and α_1 are expected to be of O(0.5). We can estimate α_1 from knowledge of the spectrum form of the surface wave configuration. Detailed estimates of α_o are found in the appendix.

Similar, but not identical, expressions for R can be obtained in the presence of swell. In this case it

can be shown that

$$\bar{\kappa} = 2\alpha'\pi I_0 \, \S^2,$$
$$I_o = \left[\int_0^\infty \Phi(\sigma)\,d\sigma\right]^{-1} \times \left[\int_0^{\sigma_t} \left(\frac{\sigma}{\sigma_p}\right)^4 \Phi(\sigma)\,d\sigma + \int_{\sigma_t}^\infty \left(\frac{\sigma}{\sigma_p}\right)^4 \Phi'(\sigma)\,d\sigma\right], \quad (3.14a, b)$$

$\alpha' \approx 0.25$, although its actual value might be somewhat higher (possibly about 0.31), as Phillips (1977) and other investigators have indicated; σ_t represents a threshold frequency above which the interactions of short waves, riding on the swell back, with the swell become significant; an expression for σ_t has been provided by Phillips (1981), viz., $\sigma_t = \{[4B(1-B)]^{-1}\}\sigma_p$, where B is the swell slope. An expression similar to (3.13b), with $\bar{\kappa}$ given by (3.14a), determines the radiative-transport term in the presence of swell. As in the absence of swell, $\bar{\kappa}$ increases with $\S^2$, a result in virtual agreement with the findings of Mitsuyasu (1985) who showed that the momentum advected away by a monochromatic (or in his terminology, regular) wave train is also proportional to the square of the wave slope, provided that momentum is equivalent to the ratio of wave energy and phase velocity.

Eqs. (3.13), and its counterpart expression in the presence of swell, give R in terms of readily obtained physical and dynamical parameters. Since the ratio ρ/ρ_a is nearly a constant (it depends primarily on the air and water temperatures) and the coefficient α_1 may be shown to be weakly dependent on §, it becomes apparent that the variations in R can mainly be attributed to those of c_p/u_*. For typical field conditions {with $c_p/u_* \cong 20-30$}, $R \cong 2.0\rho_a u_*^3$, but for laboratory waves generated in the absence of swell {with $c_p/u_* \cong 0(1)$}, $R \cong 0.2\rho_a u_*^3$. This result clearly indicates the difficulties encountered when $\rho_a u_*^3$ is taken as the total (wind) energy flux. Even under field conditions, the value of $R/\rho_a u_*^3$ is not 1.0 (although 2.0 is of order unity). Furthermore, R is not the total energy flux rate, but represents the radiative-transport of the wave energy flux. Wave energy is, in turn, only a part of the total energy transferred across the surface layer.

3.3. Wave-energy dissipation

Wave breaking is generally believed to be the dominant dissipative mechanism in a wave field at moderate and high wind speeds. In this work, we have used a version of Longuet-Higgins (1969) statistical model to calculate the fraction of wave energy losses per unit area and average wave cycle, $\tilde{\omega}$, *properly modified to account for drift current and wave crest downward acceleration effects*; $\tilde{\omega}$ is related to the rate of wave energy losses (per unit area), L, by:

$$L = \frac{\rho g \overline{\eta^2}\tilde{\omega}}{\bar{T}}, \quad \bar{T} = \frac{2\pi}{\bar{\sigma}}, \quad \bar{\sigma}^2 = \frac{\int_0^\infty \sigma^2\Phi(\sigma)\,d\sigma}{\int_0^\infty \Phi(\sigma)\,d\sigma}, \quad (3.15a, b, c)$$

where $\bar{T}$ (or $\bar{\sigma}$) is a mean wave period (or frequency). The (time) mean portion of energy losses per average wave cycle, $\tilde{\omega}$, can be expressed as

$$\tilde{\omega} = \exp\left\{-\frac{a_c^2}{2\overline{\eta^2}}\right\}, \quad a_c = \frac{g\{1-\alpha_0 u_*/c\}^2 f}{2\alpha_2\bar{\sigma}^2}$$
$$\bar{c} = \left(\frac{g}{\bar{\sigma}}\right)f^{1/2}. \quad (3.16a, b, c)$$

The coefficient α_2 {of O(1)} accounts for the fact that waves break at the crest when the local downward Lagrangian acceleration, a_L, reaches a value somewhat closer to $0.4g$ than $0.5g$. Indeed, the calculations of Longuet-Higgins (1985) have shown that, for (symmetric, steady) waves approaching the limiting form, $a_L \cong -0.39g$. For more details the interested reader should peruse Longuet-Higgins (1985); one then can calculate α_2 as being roughly equal to the ratio of $(0.5g/0.39g = 1.282)$. $f = f(\S)$ is a function accounting (indirectly) for the nonlinearities of the wave field, and represents the square of the ratio of the nonlinear and linear (average) phase speeds. For uniform steady waves of amplitude a, f may be taken as (Longuet-Higgins, 1975):

$$f = 1 + (ak)^2 + \tfrac{1}{2}(ak)^4 + \tfrac{1}{4}(ak)^6 - \tfrac{22}{45}(ak)^8 + \cdots, \quad (3.17)$$

where (ak) is the wave slope. To obtain an expression for f, in the case of a spectrum of waves, Eq. (3.17) may still be used with (ak) replaced by the average slope $(ak)_{av} = \bar{a}k_p = 2\sqrt{2}\pi\,\S$ of the wave field; here $\bar{a} = (2\eta^2)^{1/2}$. In the presence of a swell, a_c takes on a different form.

In terms of the significant slope, (3.16a) may be rewritten as

$$\tilde{\omega} = \exp\left[-\frac{\{1-\alpha_0 u_*/\bar{c}\}^4}{32\alpha_2^2\pi^2\,\S^2}\left\{\frac{\bar{\sigma}}{\sigma_p}\right\}^{-4} f^2\right],$$

$$\frac{\bar{c}}{u_*} = \left(\frac{\bar{\sigma}}{\sigma_p}\right)^{-1}\frac{c_p}{u_*} \qquad (3.18a, b)$$

or in the presence of a swell:

$$\tilde{\omega} = \exp\left[-\frac{\{(1-c_p/\bar{c})(1-B)+[(1-B)^2-\gamma(2-\gamma)]^{1/2}(c_p/\bar{c})\}^4}{32\alpha_2^2\pi^2\,\S^2(1-B)^2}\left\{\frac{\bar{\sigma}}{\sigma_p}\right\}^{-4} f^2\right],$$

$$\frac{c_p}{\bar{c}} = \frac{\bar{\sigma}}{\sigma}, \quad \gamma = u_{dso}/c_p, \qquad (3.19a, b, c)$$

where $u_{dso}(\approx \alpha_0 u_*)$ represents the value of the surface (time) mean drift at the point where the mean waveform crosses the undisturbed water level; hence $\gamma \approx \alpha_0(c_p/u_*)^{-1}$. In the appendix we describe how the representative value of the surface drift current, u_{ds}, may be connected with u_{dso}. The rate of wave energy losses, L, now becomes:

$$L = 2\pi\,\S^2\tilde{\omega}\left(\frac{\rho}{\rho_a}\right)\left(\frac{c_p}{u_*}\right)^3\left(\frac{\bar{\sigma}}{\sigma_p}\right)\rho_a u_*^3 = A_2\rho_a u_*^3. \qquad (3.20a, b)$$

Then, assuming stationary conditions and combining Eqs. (3.13), or the equivalent expression in the presence of a swell, and (3.20) we obtain:

$$W = R + L = \bar{\kappa}\left(\frac{\rho}{\rho_a}\right)\left(\alpha_1\frac{c_p}{u_*}+\alpha_0\right)\rho_a u_*^3 + 2\pi\,\S^2\tilde{\omega}\left(\frac{\rho}{\rho_a}\right)\left(\frac{c_p}{u_*}\right)^3\left(\frac{\bar{\sigma}}{\sigma_p}\right)\rho_a u_*^3 = A\rho_a u_*^3, \qquad (3.21a, b)$$

$$A = \bar{\kappa}\left(\frac{\rho}{\rho_a}\right)\left(\alpha_1\frac{c_p}{u_*}+\alpha_0\right) + 2\pi\,\S^2\tilde{\omega}\left(\frac{\rho}{\rho_a}\right)\left(\frac{c_p}{u_*}\right)^3\left(\frac{\bar{\sigma}}{\sigma_p}\right) = A_1 + A_2. \qquad (3.22a, b)$$

Thus, W represents a lower bound of the rate of the total wave-supported energy.

3.4. Energy flux into the mean drift current

Now, utilizing the boundary layer expressions mentioned previously (i.e., Eqs. 2.5–2.10 of Papadimitrakis et al. (1986a)) and the definitions of γ_M and γ_E, we derive an expression for the energy flux transferred to the (time) mean drift current. In the air surface layer, the mean rate of work done by the wind-induced drift current, $D \equiv \bar{E}_c$, can be rewritten as

$$D = \bar{M}_x u_{ds} = (\bar{M}_{xw}/\gamma_M)u_{ds} = (1-\gamma_M)^{-1}\bar{M}_{xc}u_{ds} = (1-\gamma_M)^{-1}(-\rho_a\overline{u'v'})u_{ds} \approx (1-\gamma_M)^{-1}\tau_0 u_{ds},$$

where $\bar{M}_{xc}$ represents the (time) mean current-supported momentum in the x–x direction and $-\rho_a\overline{u'v'}$ is the (time) mean turbulent (horizontal) shear stress, which in the constant stress layer proximity of the air–water interface is roughly equal to τ_o. Since $u_{ds} = \alpha_0 u_*$, D will be given as:

$$D \cong \alpha_0(1-\gamma_M)^{-1}\rho_a u_*^3 \qquad (3.23)$$

From the definition of γ_E we also obtain:

$$D \equiv \bar{E}_c = \left\{\frac{1-\gamma_E}{\gamma_E}\right\}\bar{E}_W = \left\{\frac{1-\gamma_E}{\gamma_E}\right\}\gamma_E\bar{E}_T = (1-\gamma_E)W = (1-\gamma_E)A\rho_a u_*^3. \qquad (3.24a, b, c)$$

It is now possible, by making suitable assumptions (based on available experimental evidence) regarding the relative importance of the cross-

correlations entering Eqs. (2.5–2.10) of Papadimitrakis et al. (1986a), to derive explicit expressions for the fractions γ_M and γ_E in terms of quantities that are essentially functions of the two fundamental parameters of the wave field, namely the wave age and the significant slope.

3.5. Momentum and energy partition (into waves and a mean current)

Combining (3.23)–(3.24) it can be shown that

$$\gamma_M = \frac{1-\gamma_E-\alpha_0 A^{-1}}{1-\gamma_E}, \quad \gamma_E = \frac{1-\gamma_M-\alpha_0 A^{-1}}{1-\gamma_M}. \tag{3.25a, b}$$

Since the momentum supported by a uniform wave train can be written as the ratio of the wave-supported energy and the net phase speed of the wave (Hsu et al., 1982), it can be argued that for a spectrum of waves: $\bar{M}_W = \bar{E}_W/(\bar{c}-u_{ds})$. Experimental evidence (Papadimitrakis et al., 1986a) also suggests that $\bar{M}_W \cong \bar{M}_{xw}$ because the wave-supported momentum in the vertical direction is insignificant compared to $\bar{M}_{xw}$. Then we obtain

$$\begin{aligned}\bar{M}_w \cong \bar{M}_{xw} &= \left\{\frac{1-\gamma_M}{\gamma_M}\right\}^{-1}\bar{M}_{xc} \cong \left\{\frac{1-\gamma_M}{\gamma_M}\right\}^{-1}\rho_a u_*^2 \\ &= \frac{\bar{E}_w}{\bar{c}-u_{ds}} = \frac{\gamma_E \bar{E}_T}{\bar{c}-u_{ds}} \\ &= \frac{\gamma_E W}{\bar{c}-u_{ds}} = \frac{\gamma_E A \rho_a u_*^3}{\bar{c}-\alpha_0 u_*}.\end{aligned} \tag{3.26}$$

Combination of (3.25) and (3.26) yields:

$$\gamma_M = (1-\alpha_0 A^{-1})\left\{1-\alpha_0 A^{-1}+A^{-1}\left(\frac{\bar{c}}{u_*}\right)\right\}^{-1},$$

$$\gamma_E = 1-\alpha_0 A^{-1}-\alpha_0(1-\alpha_0 A^{-1})\left(\frac{\bar{c}}{u_*}\right)^{-1}. \tag{3.27a, b}$$

It is now apparent that with γ_M and γ_E expressed as functions of c_p/u_* and §, the quantities $\bar{M}_T$, $\bar{E}_T$, $\bar{M}_w$, $\bar{E}_w$ can be expressed in terms of the same fundamental parameters. More specifically:

$$\bar{M}_{TN} = \bar{M}_T/\rho_a u_*^2 = (1-\gamma_M)^{-1},$$

$$\bar{E}_{TN} = \bar{E}_T/\rho_a u_*^3 = A, \tag{3.28a, b}$$

$$\bar{M}_{WN} = \bar{M}_W/\rho_a u_*^2 = \gamma_M(1-\gamma_M),$$

$$\bar{E}_{WN} = \bar{E}_W/\rho_a u_*^3 = A\gamma_E, \tag{3.29a, b}$$

where A is given by Eq. (3.22).

4. Results and discussion

Fig. 1 shows the variation of γ_M and γ_E fractions as a function of wave age alone, for values of c_p/u_* ranging from 0.5 to 30.0. In this plot, § does not represent an independent parameter but is expressed in terms of c_p/u_* according to the following relationships:

$$\S = \frac{\{1-\alpha_0(c_p/u_*)^{-1}\}^2}{4\pi\sqrt{2}}, \quad \text{for } c_p/u_* \leqslant 1.85, \text{ and}$$

$$\S = 31.74\times 10^{-3}(c_p/u_*)^{-0.5}, \quad \text{for } c_p/u_* > 1.85.$$

These two relationships express the ascending and descending branches of the §-c_p/u_* curve, for wind–waves generated in the absence of swell. For a detailed description of these §-c_p/u_* correlations see also Papadimitrakis (2005). Similar γ_M and γ_E curves, however, can be obtained when § is allowed to vary as an independent parameter ranging from zero to $\S_{max}$ (= 0.0356). As seen from Fig. 1, γ_M rises initially with increasing wave

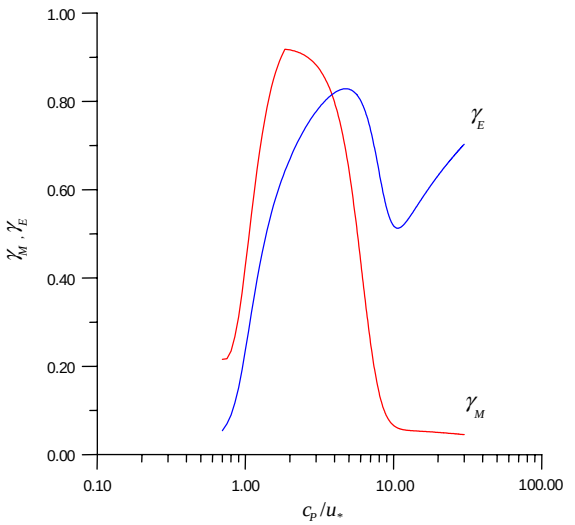

Fig. 1. Variation of γ_M, γ_E fractions (expressed by Eqs. (3.27)) as a function of wave age; § is coupled to c_p/u_*.

age for $c_p/u_* \leqslant 1.85$, but then diminishes as c_p/u_* approaches 10.0, remaining nearly constant (with a value ≈ 0.05) as c_p/u_* further increases to values close to 30.0. Such variation is very similar to the shape of the theoretical curve for the corresponding fraction γ_D derived by Donelan (1979), although the two fractions (γ_M and γ_D) are not identical. As seen from Fig. 2, when § varies independently of c_p/u_* γ_M increases with §, for $c_p/u_* =$ constant (except perhaps for $0 < c_p/u_* < 1.0$ and for very low § values). The variation of γ_M and γ_E with $\tilde{x}$ exhibits a behavior quite similar to that of Fig. 1.

Due to space limitations, figures showing swell effects on γ_M and γ_E will not be included in this work; such effects will be reported elsewhere. Yet, it was felt appropriate to include the short references describing the influence of swell on the quantities R and L, as some of the available laboratory observations have been conducted in the presence of swell (i.e. Papadimitrakis et al., 1986a) and the comparison of predicted and observed γ_M and γ_E values, under such circumstances, would be significant.

The values of γ_M and γ_E, calculated according to (3.27) using proper c_p/u_* and § values, have been

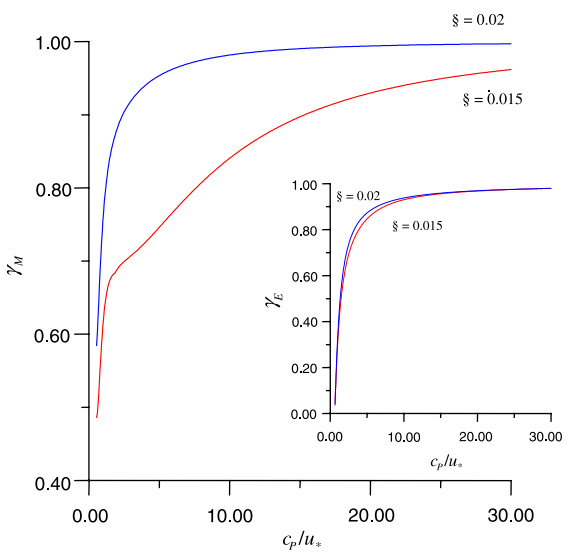

Fig. 2. Variation of γ_M, γ_E fractions (expressed by Eqs. (3.27)) with wave age and § as a parameter.

compared with the laboratory observations of Hsu et al. (1982, who also used the same definitions of γ_M and γ_E) and Papadimitrakis et al. (1986a), taken at the Stanford wind–wave facility under a variety of wind and wave conditions, and the field data of Snyder et al. (1981). Hsu et al. (1982) and Papadimitrakis et al. (1986a) have reported detailed studies of the momentum and energy transfer mechanisms across an air-water interface. In their experiments, the wind and wave fields were monitored simultaneously, under stationary conditions, with fixed and/or wave-following probes at fetches 3.46, 6.51, 9.48, 12.61, 13.00, and 15.66 m. These observations include measurements of: (i) mean and fluctuating wind velocities with a cross hot film, (ii) wind (static) pressure fluctuations with a specially designed pressure instrument (Papadimitrakis et al., 1986b), and (iii) wave height with a capacitance wave gauge. The experimental details can be found in the corresponding references.

The data of Papadimitrakis et al. (1986a) cover a range of dynamic conditions different from those of Hsu et al. (1982). To better simulate field conditions, the former authors conducted their experiments with wind blowing over 1 Hz, mechanically-generated waves. The presence of the 1-Hz wave enabled them to extend upwards the range of c_p/u_* values from 10.0 to about 37.0. In that study, it was found that the total (time) mean momentum and energy fluxes across the air–water interface are dominated by the wave-induced pressure, and that the portion of these fluxes that goes to the waves (and to the mean current) is determined by the parameter c_p/u_*. It should be noted, however, that their experiments were conducted with a single slope ($B \approx 0.1$) mechanically-generated wave and, consequently, the influence of the wave steepness (as expressed by B) on γ_M and γ_E cannot be extracted from their observations.

Snyder et al. (1981) also reported detailed measurements of the wind-stress and static pressure fluctuations in the turbulent boundary layer above ocean waves, along with simultaneous measurements of the surface wave elevation. From these observations they calculated the fraction, r_{MS}, of the momentum fluxes supported by the

waves, under a variety of wind and wave conditions. Since they defined r_{MS} as the ratio $\overline{\tilde{p}\partial\eta/\partial x}/\rho_a u_*^2$ and $\bar{M}_W \cong \bar{M}_{xw} \cong \overline{\tilde{p}\partial\eta/\partial x}$ (see Papadimitrakis et al., 1986a), it can be readily shown that $\gamma_{MS} \cong r_{MS}/(1+r_{MS})$. This γ_{MS} ratio has been compared with our predictions of γ_M, under the corresponding field conditions. It should be noted, however, that in this comparison we have used only those values of r_{MS} (from Table 9 of Snyder et al., 1981) that have not been influenced by upstream propagating reflected waves or contaminated one way or another and correspond to thermally neutral atmospheric conditions (cf. their p. 11).

Table 1 lists the predicted γ_{Mp} and γ_{Ep} values along with their experimental counterparts, γ_{Mm} and γ_{Em}, taken from Tables 2 and 3 of Hsu et al. (1982) and Table 1 of Papadimitrakis et al. (1986a), as a function of c_p/u_* and/or $\tilde{x}$. The values of wave ages encountered in the experiments of Papadimitrakis et al. (1986a) have been obtained from Table 1 of Papadimitrakis et al. (1988). The field data, r_{MS} and γ_{MS}, of Snyder et al. (1981), along with the corresponding γ_{MSp} predictions are summarized in Table 2.

As seen from Tables 1 and 2 of Hsu et al. (1982), for wind-generated waves in the absence of swell with c_p/u_* (and c_p/u_{ds}) on the order of unity, the fraction γ_M increases with increasing dimensional fetch, x, and (/or constant x but) decreasing $\tilde{x}$. In the presence of swell, with c_p/u_* (and c_p/u_{ds}) on the order of 10.0, γ_M appears to decrease with (constant dimensional fetch, x, but) increasing $\tilde{x}$, for values of c_p/u_* up to about 18, but for larger values of c_p/u_* it appears to increase again and attains values of about 0.74. The differences between the γ_M, γ_E values given by Hsu et al. (1982) and Papadimitrakis et al. (1986a) can be attributed to the dissimilar dynamic conditions governing the transfer processes between pure wind–waves and wind–waves in the presence of a longer mechanically-generated wave (representing swell in the field). The large current generated at the air–water interface, in the absence of swell, results in significant leakage of the wave-supported momentum to the drift current, in the experiments

Table 1
Wave-supported momentum and energy ratios

x	U_∞	u_*	c_p	$\tilde{x}$	$k_p\bar{a}$	§	c_p/u_*	γ_{Mm}	γ_{Mp}	γ_{Em}	γ_{Ep}
3.46	6.76	0.283	0.283	423.8	0.258	0.029	1.00	0.38	0.35	0.17	0.23
6.51	6.92	0.315	0.375	643.6	0.281	0.0316	1.19	0.53	0.48	0.34	0.32
9.48	7.02	0.326	0.460	875.1	0.256	0.0288	1.41	0.58	0.51	0.34	0.37
12.61	7.09	0.336	0.521	1095.7	0.244	0.0275	1.55	0.59	0.54	0.32	0.40
15.66	7.26	0.353	0.600	1232.9	0.226	0.0254	1.70	0.64	0.59	0.46	0.43
3.46	7.62	0.342	0.301	290.2	0.293	0.0330	0.88	0.48	0.43	0.17	0.22
6.51	7.73	0.362	0.409	487.3	0.293	0.0330	1.13	0.54	0.49	0.29	0.31
9.48	7.90	0.408	0.490	558.7	0.279	0.0314	1.20	0.64	0.67	0.13	0.34
12.61	8.01	0.400	0.580	773.2	0.255	0.0287	1.45	0.74	0.69	0.28	0.26
15.66	8.10	0.424	0.649	854.5	0.228	0.0257	1.53	0.73	0.70	0.39	0.37
3.46	8.43	0.405	0.348	206.9	0.310	0.0349	0.86	0.60	0.57	0.17	0.20
6.51	8.62	0.414	0.451	372.6	0.288	0.0324	1.09	0.59	0.55	0.33	0.31
9.48	8.81	0.475	0.556	412.2	0.267	0.0300	1.17	0.66	0.68	0.23	0.20
12.61	8.88	0.484	0.639	528.1	0.242	0.0272	1.32	0.72	0.73	0.30	0.27
15.66	8.97	0.487	0.711	647.7	0.220	0.0248	1.46	0.75	0.74	0.38	0.35
13.00	1.41	0.043	1.559	70,604.8	0.110	0.0124	36.5	0.61	0.52	0.95	0.91
13.00	1.79	0.055	1.559	41,853.7	0.110	0.0124	28.1	0.74	0.68	0.92	0.93
13.00	2.00	0.062	1.559	33,176.4	0.100	0.0113	25.1	0.75	0.72	0.90	0.86
13.00	2.31	0.072	1.559	24,329.6	0.110	0.0124	21.4	0.72	0.74	0.89	0.84
13.00	2.85	0.089	1.559	16,245.9	0.100	0.0113	17.6	0.26	0.24	0.77	0.74
13.00	3.46	0.119	1.559	8990.6	0.100	0.0113	13.0	0.43	0.45	0.76	0.72
13.00	4.02	0.156	1.559	5260.6	0.110	0.0124	10.0	0.62	0.60	0.42	0.41

Table 2
Wave-supported momentum ratios according to Snyder et al. (1981)

RUN	4	5	6	7	15	16	17	18	19	20	21	22	25	33	34	4WF	7WF	33WF	34WF
u_*		0.173	0.212	0.210	0.173	0.221	0.168	0.210	0.208	0.191	0.224	0.128	0.136	0.169	0.217	0.165	0.173	0.173	0.217	0.165
T_p		1.9	1.9	1.9	1.5	2.3	2.5	2.4	2.6	2.5	2.7	—	2.5	2.4	2.2	1.9	1.9	1.5	2.2	1.9
σ_p		0.54	0.54	0.54	0.65	0.42	0.42	0.42	0.38	0.38	0.38	0.38	0.38	0.42	0.46	0.54	0.54	0.65	0.46	0.54
k_p		1.115	1.115	1.115	1.789	0.761	0.644	0.699	0.595	0.644	0.552	0.581	0.644	0.699	0.831	1.115	1.115	1.789	0.831	1.115
$4(\overline{\eta^2})^{1/2}$		0.247	0.243	0.281	0.161	0.280	0.306	0.320	0.363	0.316	0.420	0.300	0.285	0.267	0.257	0.216	0.247	0.161	0.257	0.216
$(\overline{\eta^2})^{1/2}$		0.0618	0.0680	0.0703	0.0403	0.070	0.0765	0.08	0.0908	0.079	0.105	0.075	0.0713	0.0668	0.0643	0.054	0.0618	0.0403	0.064	0.054
c_p		2.966	2.966	2.966	2.342	3.591	3.903	3.747	4.059	3.903	4.216	4.216	3.903	3.747	3.435	2.966	2.966	2.342	3.435	2.966
c_p/u_*		17.14	13.99	14.12	13.54	16.25	23.23	17.84	19.51	20.43	18.82	32.94	28.70	22.17	15.83	17.98	17.14	13.54	15.83	17.98
$\S$		0.0110	0.0121	0.0125	0.0115	0.0085	0.0078	0.0089	0.0086	0.0081	0.0092	0.0069	0.0073	0.0074	0.0085	0.0096	0.0110	0.0150	0.0085	0.0096
$\tilde{x}$		6572	3432	3535	3091	5541	17387	7470	9947	11528	8865	53161	34206	14974	5096	10359	6572	3091	5096	7660
r_{MS}		0.70	0.56	0.60	0.20	0.64	0.77	0.77	0.72	0.81	0.91	0.32	0.35	0.61	0.44	0.47	0.49	0.46	0.51	0.58
γ_{MS}		0.41	0.36	0.38	0.17	0.39	0.44	0.44	0.42	0.45	0.48	0.24	0.26	0.38	0.31	0.32	0.33	0.32	0.34	0.37
γ_{MS_p}		0.39	0.41	0.42	0.19	0.42	0.40	0.46	0.45	0.42	0.52	0.27	0.29	0.34	0.35	0.37	0.38	0.39	0.36	0.39

of Hsu et al. (1982). As the wind speed increases (or the wave age decreases) in the experiments of Papadimitrakis et al. (1986a), γ_E decreases as it should, as a result of the decreasing ratio c_p/u_{ds} and the increasing leakage of the wave-supported momentum to surface drift current.

The variation of γ_M also may be seen in terms of the variation of the average slope of the wave field, expressed either as $k_p\bar{a}$ or $2\sqrt{2}\pi$ §. When c_p/u_* is less than about unity (≈ 1.85 when, for example, $\alpha_0 \approx 0.5$), because § increases with the wave age, γ_M increases with increasing wave slope. Yet, when the wave age is greater than about unity (1.85, i.e.) γ_M decreases with the corresponding average (and/or significant) slope. Comparison of the field and laboratory data with the predicted values of γ_M and γ_E shows the importance of c_p/u_* and § in determining the momentum and energy partition between waves and a mean drift current. In the range of c_p/u_* values from 1.0 to 30.0, the data follows the prediction curve satisfactorily. Apparently, γ_M and γ_E do not remain constant, and the waves receive more energy than the mean current at high c_p/u_* values.

Many field observations (interpreted in the light of conventional r_M ratios) indicate that most of the wind-stress is supported by the waves, suggesting that the value of 20% represents a lower bound, and that a significant portion of the (conventionally defined) momentum flux is transferred by wave drag. Field observations also show a decrease of the wave-supported momentum fraction with increasing fetch, a behavior in accord with the fact that as the wave field matures, with increasing fetch, its significant slope diminishes and, hence, the corresponding wave-supported momentum fraction (also diminishes). The laboratory findings of Banner and Peirson (1998) also support the idea that the waveform drag component becomes increasingly important, and provides the dominant contribution to the wind-stress, as the wave field matures. Their wave-associated (or wave-modulated in their terminology) part of the tangential shear stress, at the interface, also was found to be a small fraction of the total wind-stress (of about 0.05) for well-developed waves, a fact indicating again that (in these authors definition of momentum flux) the form drag

dominates the wave-coherent momentum flux. In summary, most of the features described above (for wind-generated waves at least) do not contradict the variation of our γ_M fractions with the wave age (and/or fetch), although r_M and γ_M are not identical quantities and the direct comparison of our γ_M fractions with most of the field and laboratory observations (expressed in a conventional way) may not be permissible.

It is noted that the prediction of measured γ_{Mm}, γ_{Em} ratios is improved significantly when (3.27a,b) are used in conjunction with the relevant c_p/u_* and § data set, and proper wave growth and dissipation expressions of R and L (in terms of $\bar{\kappa}$, C_d and $\tilde{\omega}$, respectively). R and L are influenced by the presence (or absence) of swell, interacting (in the former case) with the locally generated wave field. The presence of swell, and/or the interaction of higher frequency spectral components with the longer waves near the spectral peak, also enhance dissipation, by causing premature breaking, and thus affects γ_M and γ_E.

5. Total energy input

The total rate of (time) mean energy input from the wind to the water is

$$T = D + R + L = D + W \tag{5.1}$$

or in non-dimensional form:

$$\tilde{T} = \frac{T}{\rho_a u_*^3} = \frac{\alpha_0}{(1-\gamma_M)} + \bar{\kappa}\left(\frac{\rho}{\rho_a}\right)\left(\alpha_1 \frac{c_p}{u_*} + \alpha_0\right) + 2\pi\, \S^2 \tilde{\omega}\left(\frac{\rho}{\rho_a}\right)\left(\frac{c_p}{u_*}\right)^3\left(\frac{\bar{\sigma}}{\sigma_p}\right). \tag{5.2}$$

During the developing stage, (5.2) represents a lower bound of the total rate of (time) mean energy exchange between wind and sea, measured in units of $\rho_a u_*^3$.

A plot of the variation of $\tilde{T}$ with c_p/u_* (in the absence of swell), and § related to c_p/u_* through the ascending and descending §–c_p/u_* relationships, mentioned previously, is shown in Fig. 3. It is seen that as c_p/u_* increases to about 2, $\tilde{T}$ also increases, then decreases to its minimum value (≈ 2) at about $c_p/u_* = 9.5$, and finally rises again

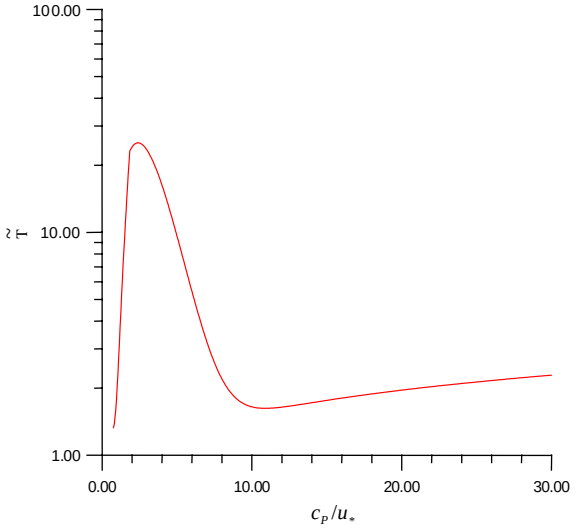

Fig. 3. Variation of $\tilde{T}$ (expressed by Eq. (5.2) with c_p/u_*, § is coupled to c_p/u_*.

slowly, as c_p/u_* approaches 30.0, to a value less than 3. For a fixed value of c_p/u_*, $\tilde{T}$ also increases rather quickly as § increases independently (Fig. 4). Yet, the efficiency of the air–sea energy exchange is limited, for both § and c_p/u_* remain bounded.

We also can determine the range of $\tilde{T}$ values for which $R \geqslant W$. Then, from the asymptotic condition $R = W$, we can obtain a threshold $(c_p/u_*)_t$ value as a function of §; that is to say we can obtain $\tilde{T}_{max}$ values (for which $R \geqslant W$) as a unique function of §. For waves generated in the presence of swell, where $\bar{\kappa}$ is given by (3.14a), $(c_p/u_*)_t$ depends on both § and B. We can generate then a family of curves (for which $R \geqslant W$), as a function of § and B as a parameter, that (again) bound $\tilde{T}$ values from above.

With the total rate of (time) mean energy exchange known, we can now explore each of the mechanisms, described previously in some detail. In Figs. 5 and 6, we have plotted both the ratios $\tilde{D}(= D/\rho_a u_*^3)$, $\tilde{R}(= R/\rho_a u_*^3)$, $\tilde{L}(= L/\rho_a u_*^3)$, and the normalized fractions $\tilde{D}_N$, $\tilde{R}_N$, $\tilde{L}_N$, which are estimated from $\tilde{D}$, $\tilde{R}$, $\tilde{L}$ by dividing the corresponding values by $\tilde{T}$, as functions of c_p/u_* alone and § coupled to it. From Fig. 5, it becomes apparent that for $c_p/u_* \geqslant 8$, $R > L$. For such values of c_p/u_*, $\tilde{T} \approx 2$–3.

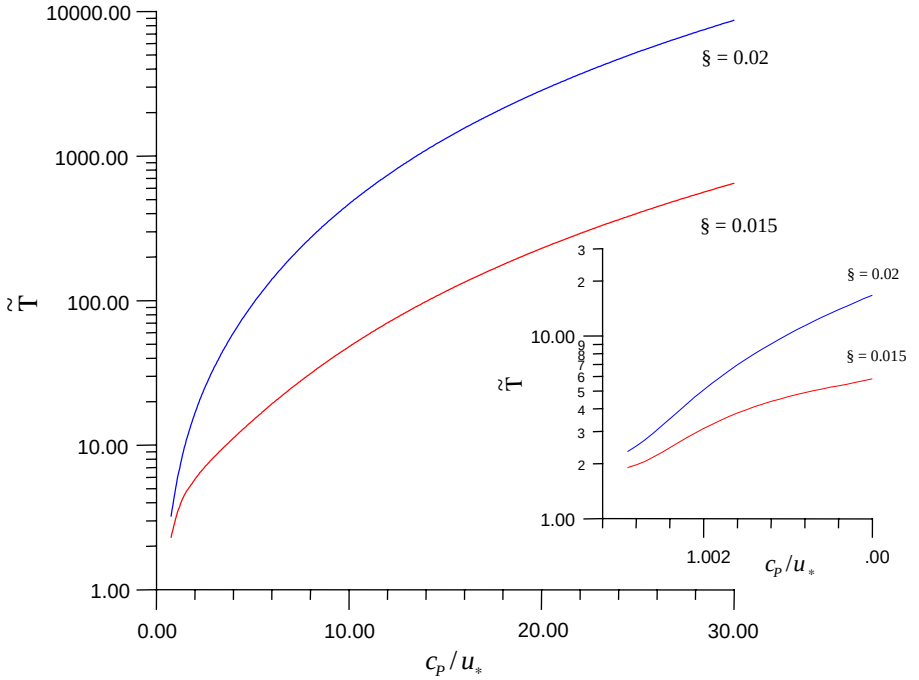

Fig. 4. Variation of $\tilde{T}$ (expressed by Eq. (5.2)) with c_p/u_* and § as a parameter.

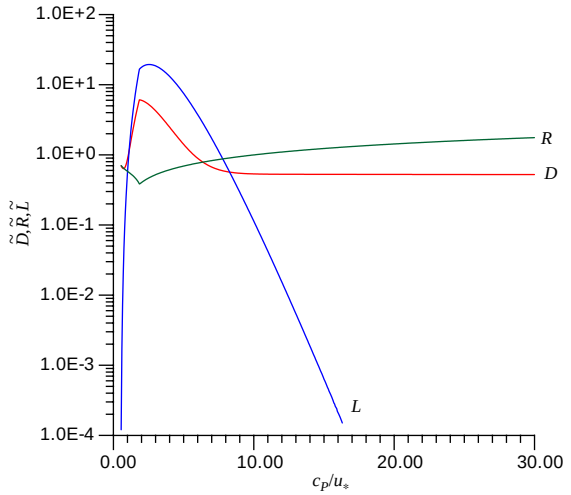

Fig. 5. Variation of $\tilde{D}$, $\tilde{R}$, $\tilde{L}$ fractions (expressed by Eq. (5.2)) with c_p/u_*; § is coupled to c_p/u_*. Red, green and blue lines represent $\tilde{D}$, $\tilde{R}$, $\tilde{L}$, respectively.

Fig. 6 also shows the reversal of roles (and of importance) between surface drift and wave growth, under field and laboratory conditions. In the laboratory, c_p/u_* is usually of O(1) and, therefore, the surface drift current receives most of the energy input (about 70–80% of the total); wave growth accounts only for about 20–30% of the energy input. This partition ratio changes under field conditions, where c_p/u_* is about 10.0–30.0. Then, wave growth receives a greater portion of the wind-energy input. Dissipation becomes important only when § > 0.013. When § reaches the value of 0.015, more than 80% of wind energy will be transferred to the mean current (and turbulence through wave breaking), thereby limiting the growth of wave steepness.

6. Conclusions

Based on: (a) an integral form of the wave-energy balance equation, (b) expressions that have resulted from the integration of boundary layer equations (in the air above water waves) governing the transfer processes across the air–sea interface, and (c) existing correlations of wave growth and

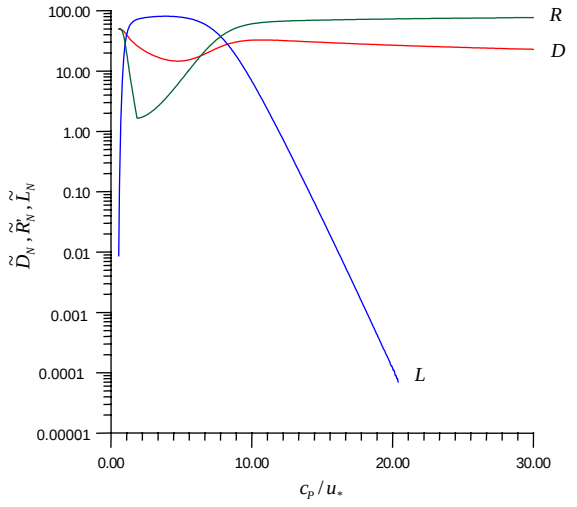

Fig. 6. Variation of $\tilde{D}_N$, $\tilde{R}_N$, $\tilde{L}_N$ fractions (expressed by Eq. (5.2)) with c_p/u_*; § is coupled to c_p/u_*. Rest as in Fig. 5.

wave-energy dissipation, we have derived a parameterization scheme (consisting of a set of explicit algebraic expressions) that allows: (i) evaluation of the total and wave-supported (time) mean fluxes of wind momentum and energy to the water motion, and (ii) the partition of total fluxes into waves and a mean drift current, during the wind–wave development stage, in terms of the wave age, c_p/u_*, and the significant slope, §, of the wave field. The parameterization scheme utilizes unified expressions that cover quite different processes, under both field and laboratory (but thermally neutral) conditions. The partition of total (time) mean fluxes is characterized by the fractions γ_M and γ_E. The agreement among observed γ_{Mm} and γ_{Em} fractions and their predicted counterparts, using the proposed parameterization expressions (i.e. Eqs. (3.27)), are considered to be satisfactory (within 10–25%), taking into account experimental uncertainties and other effects that may have contaminated the available laboratory and/or field data, one way or another.

The fraction of the wave-supported momentum, γ_M, increases initially with the wave age (and/or the non-dimensional fetch, $\tilde{x}$); but, as the wave field develops, it diminishes and remains rather constant at large wave ages (and/or $\tilde{x}$). For a fixed wave-age (and/or $\tilde{x}$), γ_M, increases with §. The corresponding wave-supported energy fraction, γ_E, shows a similar behavior for small and moderate wave ages (and/or $\tilde{x}$), but for large wave ages (and/or $\tilde{x}$) it appears to increase again.

Under laboratory (and/or field conditions), in the absence of swell, where $c_p/u_* \approx O(1)$, 70–80% of the total (time) mean wind-energy flux is supported by the drift current. Wave growth accounts for 20–30% of this energy input. When $c_p/u_* \approx 20.0$–30.0 (as usually happens in a mature wave field, in the presence of swell or otherwise), this energy partition is reversed.

Appendix. Surface-drift current considerations

According to Phillips (1977, see also Papadimitrakis et al., 1988), the Eulerian surface mean drift current, u_{ds}, may be taken as $u_{ds,\ell} - u_{ds,s} (= \alpha_0 u_*)$, where $u_{ds,\ell}$ and $u_{ds,s}$ represent the Lagrangian and Stokes (time) mean drifts. The coefficient α_0 is of O(0.5) or less, but caution must be exercised in selecting its appropriate value, as most of the surface drift current measurements are conducted in a Lagrangian frame. Experimental evidence also suggests that $u_{ds,\ell} \cong \alpha_{00} u_*$ where the coefficient α_{00} is also of O(0.5). Laboratory measurements (cf. Plant and Wright, 1980) indicate that for $0 < u_* \leqslant 30$ cm/s, $\alpha_{00} \cong 0.55$–0.60. For intermediate wind speeds, α_{00} has actually been found to increase linearly with u_*, but the opposite appears to be true for wind speeds in the range $40 \leqslant u_* \leqslant 60$ cm/s, α_{00} reaching a value ≈ 0.33 at $u_* = 100$ (cm/s). More specifically, the data of Wu (1968) and others indicate that:

$$\alpha_{00} \cong 0.53 \quad \text{for } 0 < u_* \leqslant 30 \text{ (cm/s)},$$

$$\alpha_{00} \cong 0.0175 u_* \quad \text{for } 30 < u_* \leqslant 40 \text{ (cm/s)},$$

$$\alpha_{00} \cong -0.004375 u_* + 0.875 \quad \text{for } 40 < u_* \leqslant 60 \text{ (cm/s)}. \qquad \text{(A.1a–c)}$$

Therefore, the value 0.53 (= α_{00} in general), often quoted in the literature, may not be suitable for our Eulerian calculations.

For a monochromatic wave train, the Stokes drift, $u_{ds,s}$, is given as $u_{ds,s} = (ak)^2 c$ (Kinsman,

1965), where c represents the phase speed of the monochromatic wave. For a spectrum of waves, the above simple relation maybe converted into an approximate counterpart expression of the Stokes drift with the aid of the equivalent amplitude ($\bar{a}$), associated with the sea-surface variance, and the wave number at the spectral peak frequency, k_p, viz., $u_{ds,s} \approx (2\sqrt{2}\pi\,\S)^2 c_p$. For wind-generated waves, the Stokes drift represents a small fraction of u_{ds}, being $\cong$ (0.03–0.04)u_*. Therefore, the variation of the Eulerian fraction α_0 with wind and sea state is given by (see also Papadimitrakis et al., 1988):

$$\alpha_o = \frac{u_{ds}}{u_*} = \alpha_{oo} - 8\pi^2\,\S^2\left(\frac{c_p}{u_*}\right), \qquad \S = \frac{m_0^{1/2}\sigma_p^2}{2\pi g}, \tag{A.2a, b}$$

where m_0 is the zeroth-order moment of the sea spectrum. Eq. (A.2a) states again that the Eulerian (mean) drift is the difference between its Lagrangian counterpart and the corresponding surface Stokes transport.

In the presence of swell, Phillips and Banner (1974) suggested that $\alpha_{00} \cong 0.03(U_\infty/u_*) = 0.03C_d^{-1/2}$. Then at low wind speeds {i.e. when $c_p/u_* \cong$ O(10)}, α_{00} is expected to attain values greater than 0.53–0.60, owing to the reduced surface roughness. The measurements of Cheung (1985) confirm this conclusion, yielding α_{00} values between 0.61 and 0.73 (with an average of about 0.65) for dimensionless wave speeds in the range $8 \leqslant c_p/u_* \leqslant 26$. His wave-following measurements also show clearly that α_{00} decreases with decreasing dimensionless wave speed. In the presence of swell α_{00} increases slowly with increasing wave age, $\alpha_0\{= \alpha_{00} - B^2(c_p/u_*)\}$ may either increase (for low B values) or decrease (for large B) with c_p/u_*, indicating that the (Eulerian) surface mean drift (at the zero crossing of the waveform) may become more or less effective in this case. That will depend on the combination of B and c_p/u_* values used.

In the presence of swell, the surface drift becomes a function of the phase of the swell, χ. The distribution of u_{ds} along the mean swell profile, when the latter is not breaking, is given by (Phillips, 1977)

$$u_{ds,\chi} = \{(1 - B\cos\chi)^2 - [(1 - B\cos\chi) - \gamma(2-\gamma)]^{1/2}\}c_p,$$
$$\gamma \leqslant 1 - [B(2-B)]^{1/2}. \tag{A.3a, b}$$

When $\gamma = 1 - [B(2-B)]^{1/2}$, a stagnation point is formed at the swell crest, but the surface velocity distribution (A.1a) does not allow separated flow. When $\gamma > 1 - [B(2-B)]^{1/2}$, Caponi et al. (1982) have suggested that by writing:

$$u_{ds,\chi} = \{\gamma - [1 - [B\cos\chi(2 - B\cos\chi)]^{1/2}]\}c_p,$$
$$\gamma > 1 - [B(2-B)]^{1/2} \tag{A.4a, b}$$

one can allow for wave breaking, since then, according to their calculations, a separation bubble is formed in the swell trough (cf. their Fig. 7).

Eqs. (A.3)–(A.4) provide approximate distributions of the Eulerian (time) mean surface drift in the presence of swell, under all (thermally neutral) conditions, that can be used to derive average values of the latter over the swell profile by integrating (A.3a) or (A.4a) with respect to χ, from 0 to 2π. These spatially averaged drift current values, normalized by the wind friction velocity, yield spatially averaged values of α_0 that may be greater than their counterparts at the MWL due to the modulation of surface drift by the orbital motions of the swell along the swell profile. This concept of obtaining spatially mean α_0 values could, perhaps, be applied in wind–waves generated in the absence of swell, in the sense that the dominant wave of the spectrum could also modulate the surface drift current. For providing averaged α_0 values, in the latter case, one could utilize the previously mentioned expression for α_0, derived with swell, by replacing B with the average wave slope ($2\sqrt{2}\pi\,\S$). Such spatially averaged α_0 values may be considered *more representative* of the (normalized) surface drift current along a typical surface wave profile, in between successive zero up-crossing points (*as compared with the* α_0 *values at the* MWL), and have been used in the calculations of γ_M and γ_E fractions and of the fluxes given by Eqs. (3.27)–(3.29).

References

Atakturk, S.S., Katsaros, K.B., 1999. Wind stress and surface waves observed on Lake Washington. Journal of Physical Oceanography 29, 633–650.

Babanin, A.V., Soloviev, Y.P., 1998. Field investigation of transformation of the wind wave frequency spectrum with fetch and the stage of development. Journal of Physical Oceanography 28, 563–576.

Banner, M.L., 1990. Equilibrium spectra of wind waves. Journal of Physical Oceanography 20, 966–984.

Banner, M.K., Peirson, W.L., 1998. Tangential stress beneath wind-driven air–water interfaces. Journal of Fluid Mechanics 364, 115–145.

Bye, J.A.T., Wolff, J.O., 1999. Atmosphere–Ocean momentum exchange in general circulation models. Journal of Physical Oceanography 29, 671–692.

Bye, J.A.T., Wolff, J.O., 2001. Momentum transfer at the Ocean–Atmosphere interface: the wave basis for the inertial coupling approach. Ocean Dynamics 52, 51–57.

Caponi, E.A., Fornberg, B., Knight, D.D., Mclean, J.W., Saffman, P.G., Yuen, H.C., 1982. Calculations of laminar viscous flows over a moving wavy surface. Journal of Fluid Mechanics 124, 347–362.

Chalikov, D.V., 1985. Numerical simulations of the boundary layer above waves. Boundary-Layer Meteorology 34, 63–98.

Chalikov, D.V., Makin, V.K., 1991. Models of wave boundary layer. Boundary-Layer Meteorology 56, 83–99.

Cheung, T.K., 1985. A study of the turbulent boundary layer in the water at an air–water interface. Technical Report No. 287, Civil Engineering Department, Stanford University, Stanford, CA.

Donelan, M., 1979. On the fraction of wind momentum retained by waves. In: Nihoul, J.C.J. (Ed.), Marine Forecasting, pp. 141–159.

Donelan, M.A., Hamilton, J., Hui, W.H., 1985. Directional spectra of wind-generated waves. Philosophical Transactions of the Royal Society of London A 315, 509–562.

Donelan, M.A., Drennan, W.M., Katsaros, K.B., 1997. The air–sea momentum flux in conditions of wind sea and swell. Journal of Physical Oceanography 27, 2087–2099.

Eiffler, W., 1993. A hypothesis on momentum and heat transfer near the sea–atmosphere interface and a related simple model. Journal of Marine Systems 4, 133–153.

Geernaert, G.L., Larsen, S.E., Hansen, F., 1987. Measurements of the wind stress, heat flux, and turbulence intensity during storm conditions over the North Sea. Journal of Geophysical Research 92 (C5), 13127–13139.

Grachev, A.A., Fairall, C.W., 2001. Upward momentum transfer in the marine boundary layer. Journal of Physical Oceanography 31, 1698–1711.

Hasselmann, K., Ross, D.B., Muller, P., Sell, W., 1976. A parametric wave prediction model. Journal of Physical Oceanography 6, 200–228.

Hsiao, S.V., Shemdin, O.H., 1983. Measurements of wind velocity and pressure with a wave-follower during MARSEN. Journal of Geophysical Research 88 (C14), 9841–9849.

Hsu, C.T., Wu, H.Y., Hsu, E.Y., Street, R.L., 1982. Momentum and energy transfer in wind generation of waves. Journal of Physical Oceanography 12, 929–951.

Huang, N.E., Long, S.R., Bliven, L.F., 1981. On the importance of the significant slope in empirical wind wave studies. Journal of Physical Oceanography 11, 569–573.

Jenkins, A.D., 1992. A quasi-linear eddy-viscosity model for the flux of energy and momentum to wind waves using conservation-law equations in a curvilinear coordinate system. Journal of Physical Oceanography 222, 843–858.

Kahma, K.K., Calcoen, C.J., 1992. Reconciling discrepancies in the observed growth of wind-generated waves. Journal of Physical Oceanography 22, 1389–1405.

Katsaros, K.B., Donelan, M.A., Drennan, W., 1993. Flux measurements from a SWATH ship in SWADE. Journal of Marine Systems 4, 117 132.

Kinsman, B., 1965. Wind Waves: Their Generation and Propagation on the Ocean Surface. Prentice-Hall, Englewood Cliffs, NJ.

Longuet-Higgins, M.S., 1969. On wave breaking and the equilibrium spectrum of wind-generated waves. Proceedings of the Royal Society of London A 310, 151–159.

Longuet-Higgins, M.S., 1975. Integral properties of periodic gravity waves of finite amplitude. Proceedings of the Royal Society of London A 342, 157–174.

Longuet-Higgins, M.S., 1985. Acceleration of steep gravity waves. Journal of Physical Oceanography 15, 1570–1579.

Makin, V.K., Kudryavtsev, V.N., 1999. Coupled sea surface–atmosphere. 1. Wind over waves coupling. Journal of Geophysical Research 104 (C4), 7613–7623.

Mitsuyasu, H., 1985. A note on the momentum transfer from wind to waves. Journal of Geophysical Research 90 (C2), 3343–3345.

Papadimitrakis, Y.A., 1986. On the structure of artificially-generated water wave trains. Journal of Geophysical Research 91 (C12), 14237–14249.

Papadimitrakis, Y.A., 2005. On the probability of wave breaking in deep waters, this issue [doi:10.1016/j.dsr2.2005.01.009].

Papadimitrakis, Y.A., Hsu, E.Y., Street, R.L., 1986a. The role of wave-induced pressure fluctuations in the transfer processes across an air–water interface. Journal of Fluid Mechanics 170, 113–137.

Papadimitrakis, Y.A., Hsu, E.Y., Street, R.L., 1986b. Instrument for measuring turbulent pressure fluctuations. Review in Scientific Instruments 57, 666–673.

Papadimitrakis, Y.A., Street, R.L., Hsu, E.Y., 1988. The bursting sequence in the turbulent boundary layer over progressive, mechanically generated water waves. Journal of Fluid Mechanics 193, 303–345.

Phillips, O.M., 1977. The Dynamics of the Upper Ocean. Cambridge University Press, Cambridge.

Phillips, O.M., 1981. The dispersion of short wavelets in the presence of a dominant wave. Journal of Fluid Mechanics 107, 465–485.

Phillips, O.M., Banner, M.L., 1974. Wave breaking in the presence of wind drift and swell. Journal of Fluid Mechanics 66, 625–640.

Plant, W.J., Wright, J.W., 1980. Phase speeds of upwind and downwind traversing short gravity waves. Journal of Geophysical Research 85 (C6), 3304–3310.

Sinai, Y.L., 1987. A model of interfacial stress and spray generation by gas flowing over a deep wavy pool. Journal of Fluid Mechanics 179, 327–344.

Snyder, R.L., Dobson, F.W., Elliott, J.A., Long, R.L., 1981. Array measurements of atmospheric pressure fluctuations above surface gravity waves. Journal of Fluid Mechanics 102, 1–59.

Wu, J., 1968. Laboratory studies of wind–wave interactions. Journal of Fluid Mechanics 34, 91–111.

Young, I.R., 1997. Wind Generated Ocean Waves. Elsevier, Amsterdam, The Netherlands, 288pp.

Further reading

Kitaigorodskii, S.A., 1983. On the theory of the equilibrium range in the spectrum of wind-generated gravity waves. Journal of Physical Oceanography 13, 818–827.

Makin, V.K., Chalikov, D.V., 1986. Calculating momentum and energy fluxes going into developing waves. Izvestuja Atmospheric and Oceanic Physics 22 (12), 1015–1019.